Impact response of adhesive reversible joints made of thermoplastic nanomodified adhesive

R. Ciardiello, A. Tridello, V. Brunella, B. Martorana, D.S. Paolino, G. Belingardi

Paper: Impact response of adhesive reversible joints made of thermoplastic nanomodified adhesive

THE JOURNAL OF ADHESION, None, 2017 pp: 1-30

DOI: 10.1080/00218464.2017.1354763

Impact response of adhesive reversible joints made of thermoplastic nano-modified adhesive

Authors:
R. Ciardiello[a], A. Tridello[b], V. Brunella[c], B. Martorana[d], D.S. Paolino[e], G. Belingardi[f]

[a,b,e,f] Department of Mechanical and Aerospace Engineering, Politecnico di Torino, 10129 Turin, Italy,
[a]raffaele.ciardiello@polito.it, [b]andrea.tridello@polito.it, [e]davide.paolino@polito.it,
[f]giovanni.belingardi@polito.it
[c]Department of Chemistry and NIS Research Centre, University of Torino, 10125 Torino, Italy
valentina.brunella@unito.it
[d]Centro Ricerche Fiat S.C.p.A.,Group Materials Labs, 10135 Torino,Italy
brunetto.martorana@crf.it

Corresponding Author:
Raffaele Ciardiello
E-mail address: raffaele.ciardiello@polito.it
Full postal address:
C.so Duca degli Abruzzi 24,
Department of Mechanical and Aerospace Engineering – Politecnico di Torino,
10129 – Turin,
ITALY

Abstract

The impact response of a reversible adhesive joint is experimentally assessed in the work. Joint reversibility is improved with a system that uses nano-modification of the thermoplastic adhesive used for bonding plastic components. This system, coupled with electromagnetic induction, is able to guarantee separation of the joints without any damage to the substrates. Drop dart tests at different impact velocities are carried out on neat and nano-modified bonded joints in order to compare the impact behaviour before and after the introduction of nanoparticles. Experimental results show that the impact response, assessed in terms of peak load, absorbed energy and flexural stiffness, can be affected by the introduction of nanoparticles. This work shows that adhesive nano-modified joints represent an effective and applicable solution for the reversible assembling of semi-structural components subjected to low-velocity impact loads.

Keywords: Hot-melt, impact, nanomaterials, automotive, polyolefins.

1. Introduction

In the last decades, the use of adhesives in many machinery applications has rapidly increased. Adhesive joints are often preferred to traditional mechanical fastener, for several advantages. Adhesive joints exhibit a better stress distribution compared to the traditional fasteners, if well designed [1,2]. In general, adhesives could have a higher resistance to environmental factors [3] and they are preferred to traditional fasteners when joining components made of different materials [4,5].

A wide variety of adhesives is currently available and structural and non-structural adhesives are largely adopted. Thermoset adhesives are generally employed for structural joints but, in the last years, there has been a significant increment in the use of thermoplastic adhesives, too. In some specific applications, thermoplastic adhesives are even preferable to traditional thermoset adhesives for their ease of application and for their flexibility in joining different kinds of plastic materials, even hard to bond, such as polypropylene [6]. The reason of this increase is due the adoption of many polypropylene (PP) based materials that have replaced plastics and many metals, especially in automotive sector [7].

In the automotive field, thermoplastic polyolefinic hot-melt adhesives (HMAs) are commonly adopted to assemble several interior and exterior parts. For example, this kind of adhesives are largely used to bond plastic bumper fascia to a structural plastic support [8]. Plastic bumper fascia is mainly subjected to impact loads and, in particular, to low-velocity impacts in the range [2-27 km/h], according to [9-11]. The adhesive and the relative joint are therefore frequently subjected to low velocity impacts, too. Typical examples of low velocity impacts are represented by rear vehicle impacts and debris impacts. Plastic bumpers therefore needs to be disassembled from the plastic support for maintenance operations, which could be significantly simplified if the adhesive joint can be easily separated. Simplification of the disassembly procedure is therefore a major point of interest for automotive industry.

HMAs can be separated by heating up the adhesive until the melting temperature is reached [12]. However, the melting temperature of the HMA is close to the melting temperature of the plastic substrates, and the disassembly process can introduce severe damage to the substrates. In order to set a viable solution for the disassembly procedure, innovative joining techniques have been recently proposed in the literature [13-18]. Among these, HMAs embedded with magnetic nanoparticles represent an effective solution. Nano-modification can affect the mechanical properties of the adhesive and, consequently, of the assembled part. In general, the nano-modification has a positive effect and can enhance the mechanical properties of the adhesive, especially the impact response. For instance, in [19-22] the effect of different nano-fillers on the impact response of adhesives has been investigated. In [20], it is shown that ceramic nanoparticles can significantly enhance (from 4 to15% of

increment of absorbed energy) the impact response in a speed range between 2 m/as and 8 m/s. Avila and Neto [20] showed that nano-modified epoxy resin have larger stiffness and can absorb larger energy rate during impact. Xie et al [22] showed that polyvinyl chloride (PVC) modified with nano-sized antimony trioxide particles with different weight concentrations (2.5%, 5% and 7.5%) can increase the energies needed for crack initiation and crack propagation. According to the literature results, nano-modification generally affects positively the impact response of adhesives: however, to the author's best knowledge, no experimental results are available in the literature on the impact response of nano-modified HMA. Since the HMAs currently employed in the automotive industry are mainly subjected to low velocity impact loads and the relative joint need to be frequently disassembled, the experimental characterization of the impact response of nano-modified HMAs is of utmost interest. The study of the adhesive performances under impact loading has been widely investigated. This research area gained more interest in recent years because of the increase of the use of adhesive, especially in automotive field [23].

In this work, the effect of nano-modification on the impact response of polypropylene beams bonded with a thermoplastic HMA is experimentally assessed. Drop dart tests at different impact velocities are carried out on neat and nano-modified joints. Single and repeated impact tests are performed in order to compare the impact response in terms of peak load, adsorbed energy and flexural stiffness with and without nano-modification.

2. Material and method

In this Section, the investigated material and the experimental activities are illustrated in detail. In particular, Section 2.1 describes the materials and the procedure adopted for the preparation of the adhesive joints. In Section 2.2, the experimental setup and the methodology used for the analysis of the experimental data are explained in detail.

2.1 Materials

The joints used for the experimental tests are obtained by bonding adherents made of a polypropylene copolymer with 10% in weight of talc, (Hifax CB 1160 G1, by Lyondell-Basell Industries, Houston, United States). Rectangular beams, 100 mm long with cross-section 20×3 mm, are used for the experimental tests.

The beams are bonded with a polyolefin-based HMA (Prodas by Beardow Adams, Milton Keynes, United Kingdom), a copolymer of polypropylene and polyethylene [16]. The nano-modified adhesive is prepared by using a hot plate for melting the neat adhesive and by adding 10% in weight of iron oxide particles with size smaller than 50 nm (Fe_3O_4 by Sigma-Aldrich, Saint Louis, United States). Following a procedure commonly adopted in the literature for HMA [6,9,11,13], the pellets were melted together at 190°C, using the hot plate. At 190°C, the viscosity of the adhesive was low enough to easily mix the particles into the adhesive by mean of a glass road. The iron oxide nanoparticles were added gradually and mixed together with the adhesive.

Joint preparation is performed with a hot-melt gun (Figure 1a) and an assembly device (Figure 1b) which permits to control the thickness of the adhesive joint.

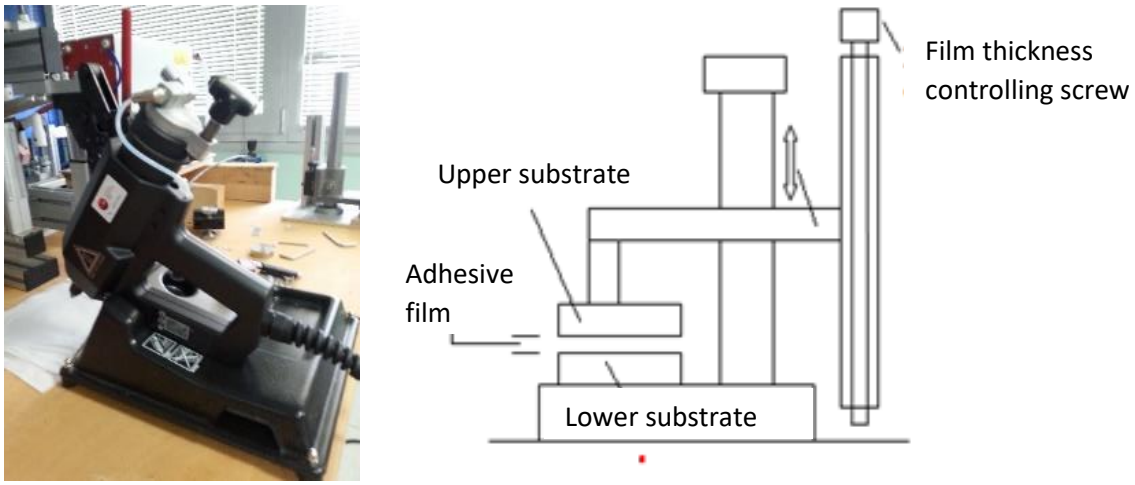

a) b)

Figure 1: Instrumentation used for the joint preparation: a) hot melt gun; b) assembly device [16].

Nominal thickness of the adhesive layer is $1\ \mathrm{mm}$. As shown in Figure 1b, a film-thickness controller screw was used to fix the thickness of the adhesive layer. Firstly, the adherent (lower substrate in Figure 1b) was fixed on the lower base of the assembly device. Then, the HMA at high temperature was uniformly spread through the hot melt gun over the lower substrate. An amount of adhesive larger than necessary was used to ensure that the lower substrate was completely covered. Then, the upper adherent (upper substrate in Figure 1b) was placed on the hot adhesive. In order to remove the adhesive in excess, a weight of $(3.5\ \mathrm{kg})$ was placed on the support of the upper adherent. This procedure allows to remove the adhesive in excess until the required adhesive thickness is reached.

The thickness of each joint was measured and was found to be constant along the joint length, with a variation smaller than $0.05\ \mathrm{mm}$. When the adhesive solidified, the adhesive in excess was removed mechanically through the use of a cutter.

Figure 2 shows a bonded joint used for the experimental tests. The nominal dimensions of the joint are also reported. All the reported dimensions are in millimetres.

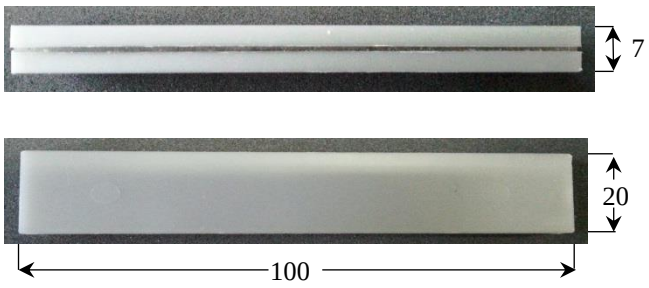

Figure 2: Bonded joint used for the experimental tests. Dimensions in mm.

Before the experimental tests, the dispersion of the iron oxide within the plastic matrix is verified by using a Scanning Electron Microscope (SEM). SEM analysis were carried out using a Carl-Zeiss EVO50. The electronic high tension used was 20 kV and the secondary electron emission was used as signal. The specimens were properly coated with gold in order to have better images. The sample for the SEM observation was obtained by gradually heating a bonded joint at 80 °C, quite below the softening point of the HMA, and thereafter by easily separating the joint through a sharp cutter. The SEM analyses were conducted on the smoothest area found through visual inspection. Two specimens were used for the SEM observation.

Figure 3 shows a representative SEM image at 500X magnification of the nano-modified adhesive. In this figure the biggest white shining spot are due to the presence of some deposed residual, since the adhesive is sticky.

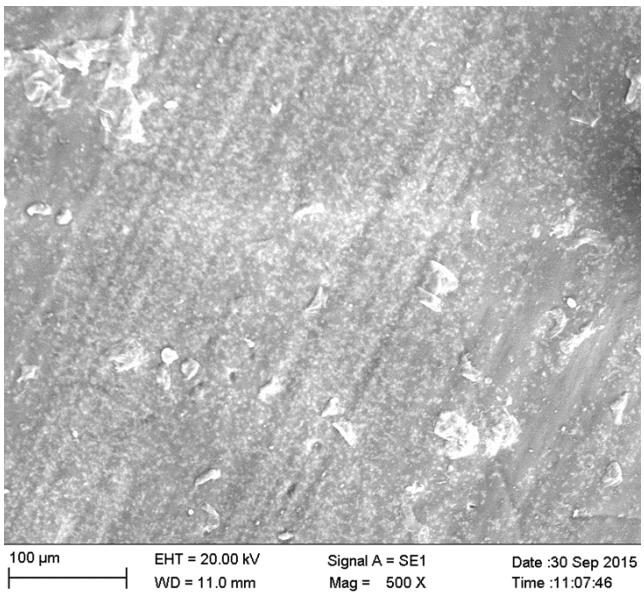

Figure 3: Representatitve SEM image at 500X of the modified adhesive: black boxes show the regions without nano-particles.

According to Figure 3, the tiny white spots are the iron oxide nanoparticles embedded in the HMA matrix. The distribution of the fillers within the adhesive is almost uniform: areas with no particles, measured thorugh digital image processing, is equal to 854.1 μm^2 and represent the 0,15% of the investigated area.

Figure 4a and 4b show SEM images of the modified adhesive at 5000x and at 10000x, respectively.

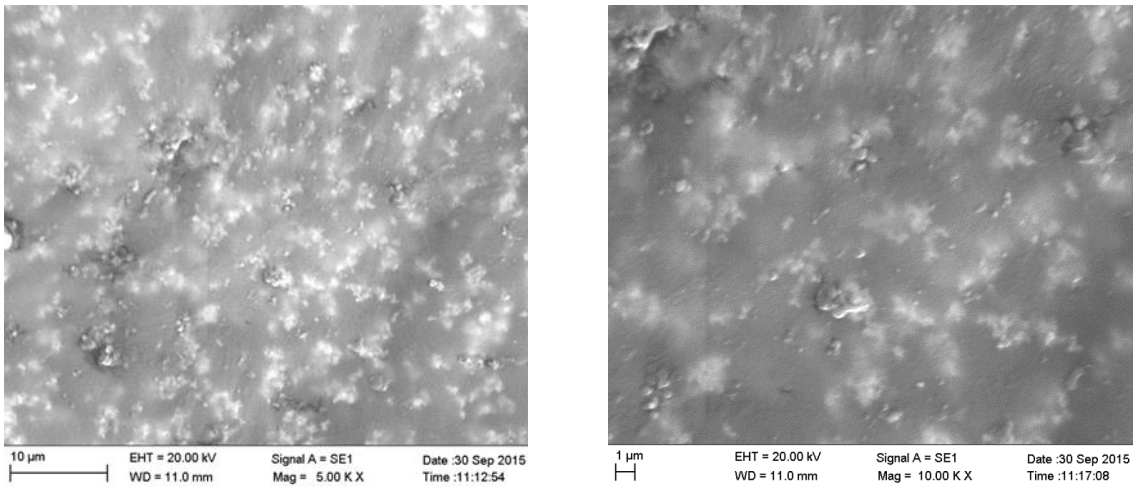

a) b)

Figure 4: SEM images of the nano-modified adhesive: a) 5000x image; b) 10000x image.

According to Figure 4a and 4b, nanoparticles tend to form small aggregates well distributed. The aggregate dimension was verified at 15 different locations in Figure 4a. In particular, the average particle size was found to be equal to 0.86 µm, with limited scatter (standard deviation of 0.41). The presence of this small aggregate is attributed to the nature of the particles that before mixing display a tendency to aggregate as shown in figure 5. Figure 5 shows the Atomic Force Microscope (AFM) analysis of the particles used in this work. The microscope, by Veeco Digital Instrument (Santa Barbara,

USA), was used in tapping mode and with a Si_3N_4 cantilever. Figure 5 displays that the single particles dimensions are lower than 55 nm but they arise as clusters and their size are very close to the one measure in the adhesive matrix. The lower cluster is around 78 µm, according to the scale of the figure.

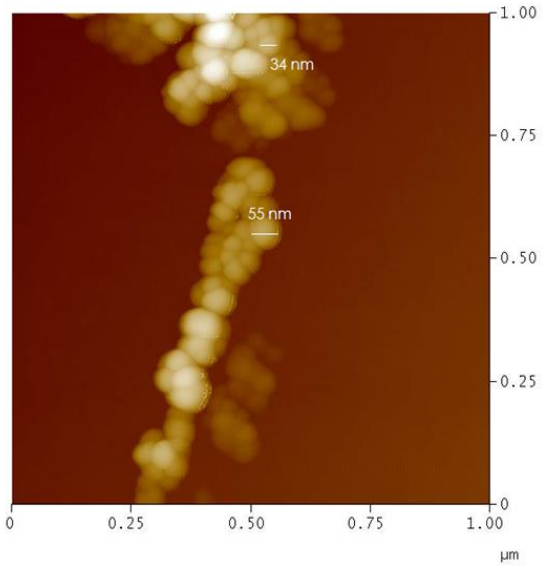

Figure 5: AFM of the iron oxide nano-particles [14].

2.2 Flexural elastic modulus

Flexural elastic modulus of neat and nano-modified joint is assessed through the Impulse Excitation Technique (IET). According to the ASTM standard [24], the bonded joint is supported at the two nodal points of the first modal shape for driving the flexural mode of vibration. Through a small hammer with a spherical head (4 mm diameter), the joint is hit in the centre of the bar in order to excite the bending mode of vibration. A microphone is used to acquire the vibration amplitude at the free edge of the joint. The signal coming from the microphone is acquired by using a Data Acquisition Card (DAQ) and used to assess the frequency response through the application of the Fast Fourier Transform algorithm. The flexural modulus is finally obtained according to [24]. Figure 6 shows the IET system used for the assessment of the flexural elastic modulus, described above.

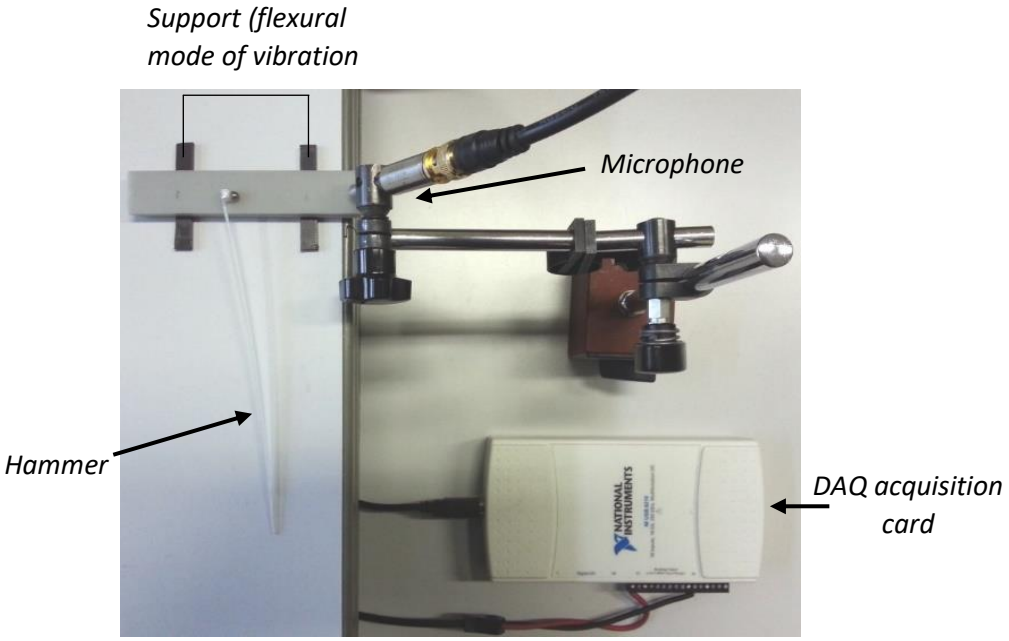

Figure 6: IET system for assessing the flexural elastic modulus.

IET tests are carried out on two neat and two nano-modified joints. Three measurements for each joint are performed. Figure 7 shows representative frequency spectra obtained with the IET tests on the neat (Figure 7a) and on the nano-modified joints (Figure 7b). The small boxes inside the Figures show a magnification of the peak region.

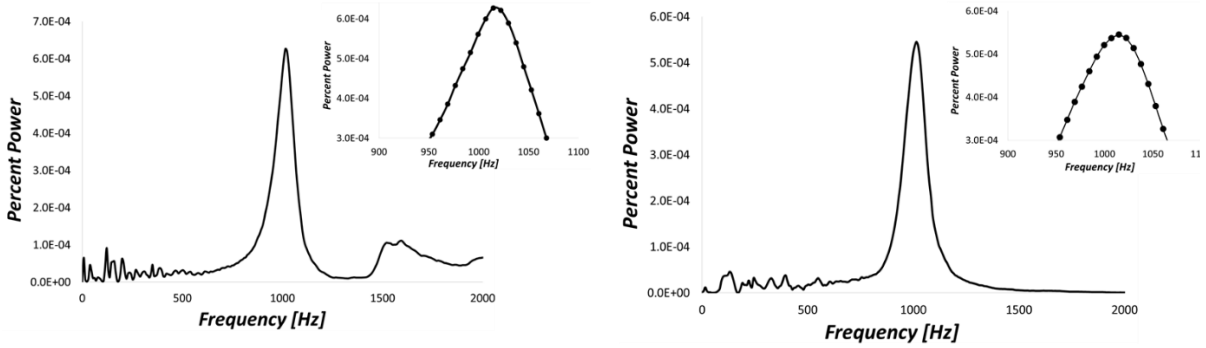

a) b)

Figure 7: IET spectra for the investigated joints: a) neat joint; b) nano-modified joint.

A negligible scatter, smaller than $7\ \mathrm{Hz}$, is found in the spectra obtained experimentally. The flexural modulus is found to be in the range $[1.9\ ;\ 2.0]\ \mathrm{GPa}$ for the neat joint and in the range $[1.9\ ;\ 2.1\ ]\ \mathrm{GPa}$ for the nano-modified joint. Therefore, the nano-modification does not significantly affect the flexural elastic modulus.

2.3 Impact test setup

For the assessment of the impact response, impact tests are carried out using a free-fall drop dart testing machine (CEAST 9350 FRACTOVIS PLUS) equipped with a $12{,}7\ \mathrm{mm}$ hemispherical impactor tup. The impact speed is obtained by varying the drop height. Moreover, for each impact test, the impact speed is measured by using a magnetic encoder. The encoder measures the speed of the impactor just before it comes into contact with the specimen. Therefore for each test, the actual speed before the impact is measured in order to accurately compute the impact energy. The speed signal is also used as a trigger to start the acquisition of the load signal, in order to reduce the amount of acquired data. The joints to be tested are clamped at both ends by a mechanical clamping system which ensures a uniform pressure all over the clamping area, as shown in Figure 8.

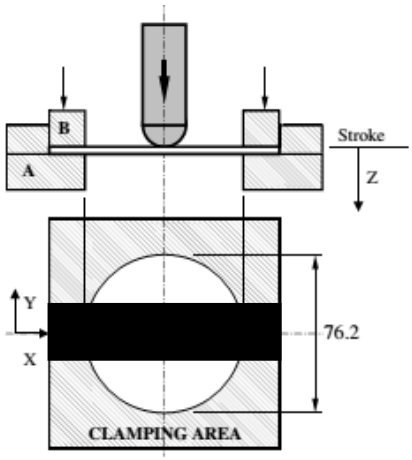

Figure 8: Clamping system for the impact tests. In black, the clamped specimen.

Load signal is acquired by using a piezoelectric load cell (203B by PCB Piezotronics, Depew, United States) with a sample rate of $1\ \mathrm{MHz}$. According to [25,26] and by considering the energy balance equation during the impact, displacement-time curve is obtained by integrating twice the acquired load signal with respect to time. Through an additional integration of the load with respect to the displacement, the adsorbed energy can be finally obtained.

Initial experimental plan envisaged to use two different velocities: 10 m/s, which gives, without any additional mass, an energy of 368 J, and 5 m/s with the same energy, through additional masses. Tests performed at 5 m/s gave repeatble results as can be seen in Figure 9. On the other hand, tests performed at 10 m/s did not give acceptable results, due to the slippage of specimens in the clamping fixture. Figure 9 shows the trend of the test performed at 10 m/s, together with the tests run at 5 m/s. The 10 m/s test exhibits a significant decrement of the force signal, in the displacement range from 5 mm (beginning of slippage) to 31 mm (end of the test). After the 10 m/s test specimen was bent but not perforated. For these reasons, a lower velocity, equal to 8 m/s, was chosen for the subsequent tests. Tests at 8 m/s still permitted to evaluate the effect of strain-rate in the limited range from 5 m/s to 8 m/s. Tests at 8 m/s gave repeatable results, as can be seen in Figure 11 in the next section.

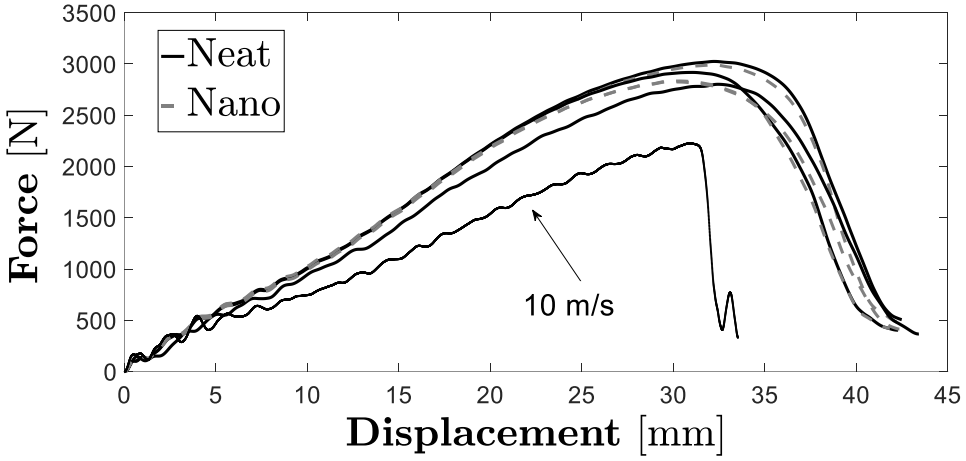

Figure 9: Force-displacement curves at 5 m/s and 10 m/s.

The behaviour of the joint is also investigated in a different damage condition, with repeated impacts at low energy that do not lead to perforation even for a high number of impacts. From the perforation tests, it was possible to evaluate the maximum perforation energy of the joint. In order to assess the behaviour of the joint under repeated impacts, twenty impacts with an energy of 8 J (around 10% of the value of the perforation energy) are then carried out. The chosen impact energy guarantees a low damage accumulation impact after impact, according to [27].

Perforation impact tests on neat and nano-modified joints are performed at an impact speed of $5\ \mathrm{m/s}$. The effect of velocity is investigated by testing the joints at a larger speed of 8 m/s with the same impact energy.

Repeated impact response is also experimentally evaluated. To this aim, ten repeated impact tests at low energy (8 J) are performed. Residual elastic modulus after the last impact is evaluated through the IET. The experimental activity is summarized in Table 1.

Table 1: summary of the experimental impact activity

	Impact velocity [m/s]	*Impact energy [J]*	*Number of repetitions*	*Impact mass [kg]*
Perforation tests	5	368	3	29.4
	8	368	3	11.5
Repeated impacts (10 impacts)	1.5	8	2	7.4

3. Experimental results: Perforation tests

Perforation experimental tests are carried out at an impact energy significantly larger than the estimated perforation energy of the specimen.

During each perforation test, bars are split into two parts with almost equal length. Figure 10 reports an example of a joint after the perforation impact. Failure modes of neat and nano-modified joints are found to be very similar and no difference is found between failure modes in impact tests performed at different velocities.

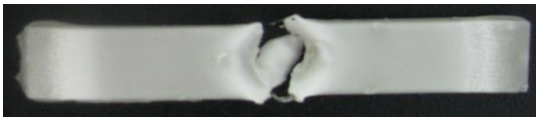

Figure 10: An example of a neat joint after perforation.

Experimental data are analyzed with a script written in Matlab®. Figure 11 shows the force-displacement and the energy-displacement curves for the neat and nano-modified joints tested at $5\ \mathrm{m/s}$ (Figures 11a and 10c) and $8\ \mathrm{m/s}$ (Figures 11b and 10d).

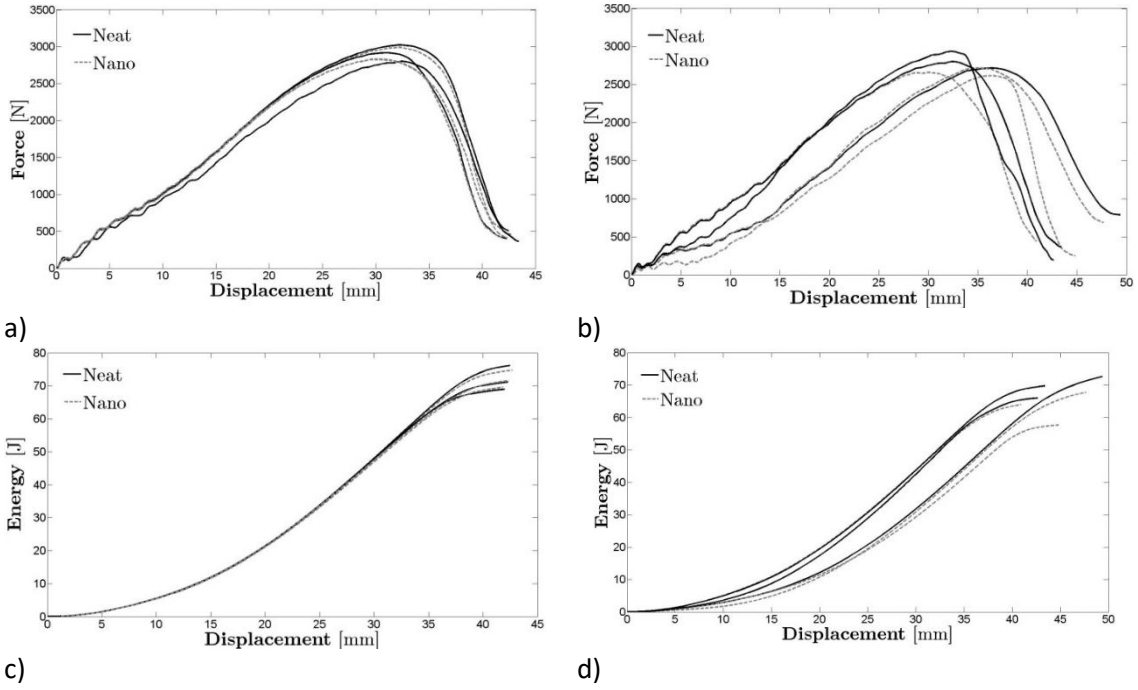

Figure 11: Perforation curves: a) Force-displacement at $5\ \mathrm{m/s}$; b) Force-displacement at $8\ \mathrm{m/s}$; c) Energy-displacement at $5\ \mathrm{m/s}$; d) Energy-displacement at $8\ \mathrm{m/s}$.

According to Figure 11, the impact responses of neat and nano-modified joints are quite similar: curves follow same qualitative trends. Repeatability is good and curves are concentrated within a limited region.

Table 2 summarizes the experimental results obtained after the perforation impact tests on the neat and nano-modified bonded joints. In particular, maximum and minimum values of peak force, absorbed energy and stiffness are reported in Table 2. According to [25], the flexural stiffness is evaluated as the slope of the initial straight line in the force-displacement curve.

Table 2: Experimental dataset for the perforation impact tests.

	Impact velocity [m/s]	*Peak force [N]*	*Energy [J]*	*Stiffness [N/mm]*
Neat	5	[2907;3024]	[69;76]	[107.4;107.7]
	8	[2717;2917]	[66;74]	[99; 112]
Nano-modified	5	[2881;3023]	[69;74]	[103;107]
	8	[2787; 2832]	[59; 69]	[101;107]

According to Figure 11 and Table 2, the experimental results for the nano-modified adhesive show a larger scatter. The introduction of nano-particles can locally modify the mechanical properties of the adhesive and affect experimental response (SEM analysis in Section 2.1).

A statistical analysis is therefore carried out in order to evaluate if the nano-modification significantly influences the impact response of the investigated thermoplastic bonded joint. The effect of velocity is also investigated both for the neat and the nano-modified bonded joint. Analysis of Variance (ANOVA) is used to statistically compare the data. In the following section, the ANOVA analysis is applied to peak force, absorbed energy and stiffness. Two factors are investigated (i.e., nano-particles and velocity), with three replications for each treatment combination. A 95% and 90% significance level is considered in the analysis.

The resulting ANOVAs are reported in the following sections. The main parameters used in the calculation of the ANOVA are reported in each table. Sum of Squares (SS), Degrees of Freedom (DOF), Mean Squares (MS) and Fisher ratios (F) are computed from the experimental data and reported in each table, together with the 95-th and 90-th percentile of the Fisher distribution (F95%). In the analysis, sum of square represents the deviation from the mean and it is calculated as the sum of the

square of the differences from the mean. The DOF is the number of levels minus one. The ratio between SS and DOF gives the MS, which represents the variations among sample means. For the assessment of the influence of the considered factors, the Fisher test is performed under the null hypothesis that the mean taken into account are equal. The Fisher ratio is computed from the experimental data as the ratio between MS and the MS error. *F95% and F90%* ratios are considered into the analysis since they are the characteristic values which confirm the significance of the results obtained in this work. The applicability of ANOVA (population normality and variance heterogeneity) was verified through statistical tests.

3.1 Peak force

Table 3 reports the results of the ANOVA for the peak force.

Table 3: ANOVA for the peak force.

Source	***SS***	***DOF***	***MS***	***F***	***F95%***	***F90%***
Nano-particles	30070	1	30070	4.39	5.32	3.46
Velocity	40751	1	40751	5.95	5.32	3.46
Interaction	5071	1	5071	0.74	5.32	3.46
Error	54811	8	6851			
Total	130704	11				

According to Table 3, for the investigated range of velocities, the velocity and the introduction of the nanoparticles affects the peak force when a 90% significance level is considered. The velocity affects the impact response also with a 95% significance level. On the other hand, the interaction between the velocity and the introduction of nano-particles is not affecting the impact response for the peak force.

3.2 Absorbed energy

Table 4 reports the results of the ANOVA for the absorbed energy.

Table 4: ANOVA for the absorbed energy.

Source	***SS***	***DOF***	***MS***	***F***	***F95%***	***F90%***
Nano-particles	36.75	1	36.75	2.20	5.32	3.46

Velocity	60.75	1	60.75	3.64	5.32	3.46
Interaction	24.08	1	24.08	1.44	5.32	3.46
Error	133.33	8	16.66			
Total	254.91	11				

Table 4 shows that nano-particles do not affect the absorbed energy when a 90% and 95% significance level is considered. On the other hand, the velocity affects the impact response when a 90% significance level is considered. The interaction between the two parameters does not affect the impact response, for the adsorbed energy.

3.3 Stiffness

Table 5 reports the results of the ANOVA for the stiffness.

Table 5: ANOVA for the stiffness.

Source	***SS***	***DOF***	***MS***	***F***	***F95%***	***F90%***
Nano-particles	13.19	1	13.19	0.81	5.32	3.46
Velocity	21.05	1	21.05	1.29	5.32	3.46
Interaction	0.32	1	0.31	0.02	5.32	3.46
Error	130.07	8	16.25			
Total	164.64	11				

Finally, the ANOVA on the stiffness confirms that no statistical difference exists before and after the introduction of the nano-particles and the velocity does not affect the impact response when both F95% and F90% are considered.

3.4 Repeated impacts

The experimental response to repeated impacts is analyzed in this Section. Experimental data are assessed according to the methodology described in Section 2.2. Figure 12 shows the normalized peak force (F_{max} normalized with respect to the peak force at the first impact, $F_{max,1}$) versus the impact number.

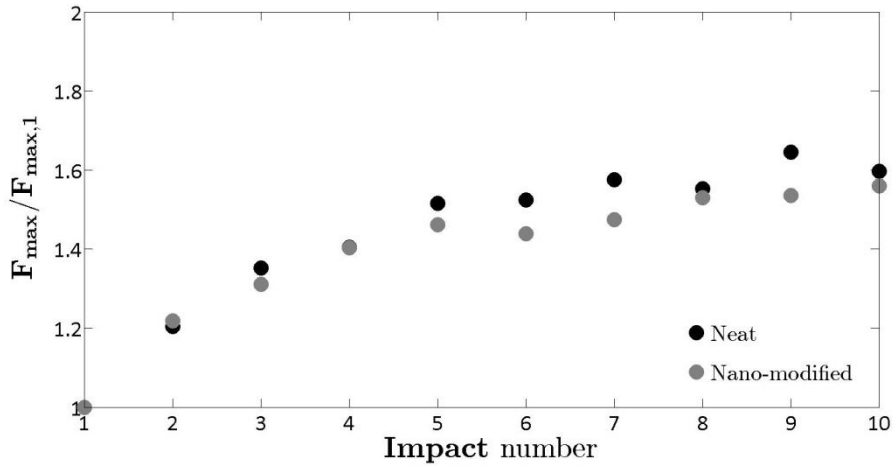

Figure 12: Normalized peak force with respect to the impact number.

According to Figure 12, the peak force trends are almost similar for the neat and nano-modified joints. In particular, the peak force tends to increase in the first five impacts, while it keeps constant after the sixth impact. The degradation of the elastic modulus after the repeated impact tests is experimentally assessed through the IET. IET is applied to the damaged neat and the nano-modified joints, with the same configuration described in Section 2.2. Figure 13 shows representative frequency spectra obtained with the IET tests on a damaged neat (Figure 13a) and on a nano-modified joint (Figure 13b).

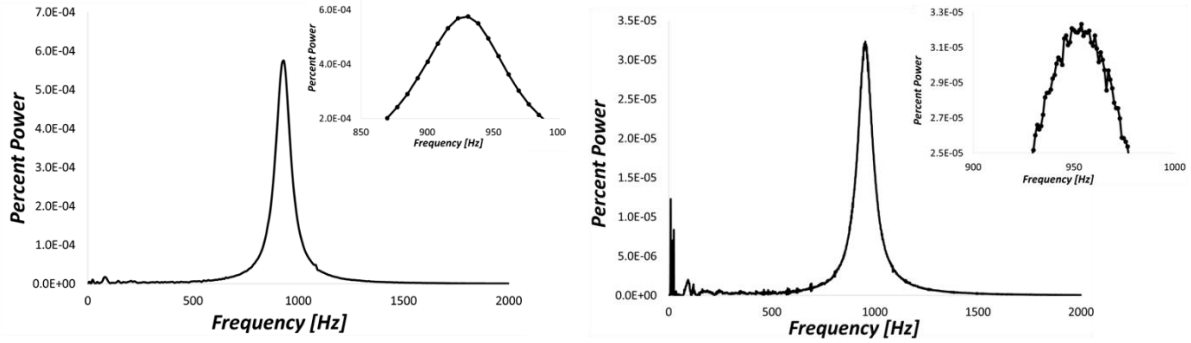

a) b)

Figure 13: IET spectra for the investigated damaged joints: (a) neat joint; (b) nano-modified joint.

According to Figure 13, the resonance peak decreases due to the damaged introduced by the repeated impacts: in Figure 4 the resonance peak is about 1015 Hz for both joints, whereas, after ten repeated impact tests, the resonance peak decreases to about 950 Hz. For each damaged joint, three measurements are performed. The peak for the nano-modified joint show a larger noise, probably due to a non-uniform distribution of the particles within the adhesive after the impact. However, the peak is clear and the larger noise does not affect the computation of the residual elastic modulus.

Table 6 compares the elastic modulus before and after the repeated impact tests. E_f is the flexural elastic modulus before the repeated impact tests. $E_{f,r}$ is the residual elastic modulus joints after the last impact. Minimum and maximum moduli are reported in Table 6.

Table 6: Flexural elastic modulus of the bonded joints before and after the repeated impact tests.

	E_f [GPa]	$E_{f,r}$ [GPa]

Neat	[1.9 ; 2.0]	[1.3 ; 1.4]
Nano-modified	[1.9 ; 2.1]	[1.4 ; 1.5]

According to Table 6, the decrement of the elastic modulus is equivalent for the neat and the nano-modified joint. After ten impacts, the average decrement is about 30%. Therefore, the introduction of the nano-particles does not influence the repeated impact response of the investigated joint.

4. Conclusions

The objective of this work was to evaluate the impact response of a nano-modified thermoplastic adhesive, which is currently used in the automotive field for parts subjected to impulsive loads. Single and repeated impact tests were carried out on neat and nano-modified (with iron oxide) joints.

Experimental results and ANOVA show that the introduction of a 10% in weight of nano-particles influences the impact response of the joint only for the peak force and using a 90% significance level. Obtained values of peak force, perforation energy and flexural stiffness are very similar for the neat and the nano-modified joints. Furthermore, tests performed at different impact velocities showed that the effect of the velocity is more evident when the peak force and the adsorbed energy are considered. Finally, the reduction of the flexural modulus after ten low energy impacts was significant but equivalent in the two joint types.

The introduction of nano-particles in the tested thermoplastic adhesive is an interesting practice, because it allows for an easier dismantling when required (for repairing or recycling) and it has also the potentiality to reduce the process time if a suitable equipment is designed. Reversible adhesive nano-modified joints represent a valid and effective solution for assembling-disassembling structural components even in the cases when they are subjected to impulsive loads.

References

[1] Changa, B., Shi, Y., and Dong, S. J. Mater. Process. Technol. 87,230–236 (1999).

[2] Belingardi, G., and Chiandussi G. Int. J. Adhes. Adhes. 24,423-439 (2004).

[3] Pizzi, A., and Mittal, K. Handbook of Adhesive Technology (Marcel Dekker, Inc, New York, 2003). 2nd ed.

[4] Structural bonding of lightweight cars [Internet]. 2010 Available from: http://www.dowautomotive.com/pdfs/Structural_Adhesives_Brochure.pdf. [Accessed: 2016-06-01].

[5] Mallik P., Materials, Design and Manufacturing for Lightweight Vehicles (Woodhead publishing, Dearborn, 2010).1st ed., Chap. 10 Pp. 384.

[6] Belingardi, G., Martorana, B., Brunella, V., and Ciardiello, R. Thermoplastic adhesive for automotive applications. Adhesives-application and properties (INTECH, Rijeka, 2016). 1st. ed. Chap 13 p.341-362.

[7] Polypropylene Compounds for Automotive Applications. [Internet] 2010. Available from:http://www.sumitomochem.co.jp/english/rd/report/theses/docs/20100100_a2g.pdf [Accessed: 06-05-2016]

[8] Ebnesajjad, S. Adhesives technology handbook (William Andrew Inc., Norwich, 2008) 2nd ed. Chap. 1 p. 1-5.

[9] Nishimura, N., Simms, C.K., and WoodImpact, D.P. Accid Anal Prev 79,1–12 (2015).

[10] Brach, R. Modeling of Low-Speed, Front-to-Rear Vehicle Impacts, SAE Technical Paper 2003-01-0491 (2003), doi:10.4271/2003-01-0491.

[11] Han., I. Proc. Inst. Mech. Eng. D J. Automob. Eng. 230(4),554–563 (2016).

[12] Ciardiello, R., Belingardi, G., Martorana, B., Fondacaro, D., and Brunella, V. ECCM, Proc. Int. Conf. Compos. Mater. 2016.

[13] Skeist, I. Handbook of adhesives. (Van Nostrand Reinhold,New York, 1990) 3rd. ed. p. 931.

[14] Verna, E., Cannavaro, I., Brunella, V., Koricho, E.G., Belingardi, G., Roncato, D., Martorana, B., Lambertini, V., Neamtu, V.A., and Ciobanu, R. Int. J. Adhes. Adhes. 46, 21-25. 2013.

[15] Zinn, S., and Semiatin, S. Heat treat. Mag. 1988 32-41.

[16] Koricho, E., Verna, E., Belingardi, G., Martorana, B., and Brunella, V. Int. J. Adhes. Adhes. 68,164-181. 2016.

[17] Banea, M.D., da Silva, L.F.M., Campilho, R.D., and Sato, C. J. Adhes. 90,16–40. 2014.

[18] Banea, M.D., da Silva, L.F.M., Carbas, R.C.J., and de Barros, S. J. Adhes. 1-15 (2016). (http://dx.doi.org/10.1080/00218464.2016.1199963).

[19] Lin, J., Chang, L.C., Nien, M.H., and Ho., H.L. Compos. Struct. 74,30–36 (2006).

[20] Avila, A.F., and Neto, A.S. Int. Mech. Eng. Congress. Expo. 15838,643-650 (2006).

[21] Avila, A.F., Carvalho, M.G.R., Dias, E.C., and a Cruz, D.T.L. Compos. Struct. 92,45–751 (2010).

[22] Xie, X., Li, R., Liu, Q., and Mai, Y. Polymer 45,2793–2802 (2004).

[23] Machado, J.J.M., Marques, E.A.S., and da Silva, L.F.M. j. Adhes. 1-32 (2017). (DOI:10.1080/00218464.2017.1282349)

[24] ASTM Standard E1876-09. Standard test method for dynamic Young's modulus, Shear modulus, and Poisson's ratio by impulse excitation of vibration. (ASTM International, West Conshohocken, 2009).

[25] Belingardi, G., and Vadori, R. Compos. Struct. 61,27–38. 2003.

[26] Belingardi, G., Cavatorta, M.P., and Paolino, D.S. ICCM, Proc. Int. Conf. Compos. Mater. 35,609–619, 2008.

[27] Belingardi, G., Cavatorta, M.P., and Paolino, D.S. Compos. Sci. Technol. pp. 69, 1693-1698. 2009.